



# Studying the destruction of pollutant in the presence of photocatalysts based on MWCNTs with controlled values of TiO<sub>2</sub> nanoparticles

Sedigheh Abbasi<sup>1</sup>

Received: 20 November 2022 / Accepted: 27 February 2023 / Published online: 17 March 2023  
© The Author(s) 2023

## Abstract

The main goal of the present research is the synthesis of new photocatalysts to reduce the amount of organic pollutants in aquatic environments. For this purpose, the amount of TiO<sub>2</sub> nanoparticles in the synthesized samples containing MWCNTs is controlled to synthesize two types of photocatalysts named as MCT#1 and MCT#2. Samples characterizing using XRD reveal that the TiO<sub>2</sub> nanoparticles have a combined phase of rutile and anatase. So that in both of photocatalysts, the percentage of anatase phase is higher than rutile. The analysis of the degradation rate demonstrates that intensification level of TiO<sub>2</sub> nanoparticles in MCT#2 compared to the MCT#1 leads to enhancement of photocatalytic activity of MCT#2. Design of experiment results shows that the destruction amount of MO is affected by irradiation time and pH. Based on ANOVA study, it is observed that both factors have a significant effect on reducing of MO concentration. Analyzing the results based on Duncan's multiple range test at  $\alpha=0.05$  confirm that all the studied levels of the main parameters have a logical influence on MO destruction. Meanwhile, it can be deduced that the most and the least of destruction is observed at pH = 7 and pH = 3, respectively.

**Keywords** MWCNTs · Anatase TiO<sub>2</sub> · Rutile TiO<sub>2</sub> · ANOVA · Photocatalysts · Design of experiment

## Introduction

Photocatalytic decomposition of dye contaminants from water systems has great deal of interest due to low cost, high removal efficiency, easy procedure and generation of nontoxic products such as water and carbon dioxide (Abbasi 2018, 2019). The photocatalytic decomposition of dye pollutants is based on the electron excitation in the common semiconductors such as SnO<sub>2</sub>, TiO<sub>2</sub> and ZnO (Abbasi 2020, 2021a; Zhou et al. 2013; Zhu et al. 2015). The irradiation of applied semiconductors with more energy than the band gap causes to the electron incitement and migration of excited electrons from valence band (VB) to the conduction band (CB). As a results of electrons transmittance between VB and CB, the unstable electron–hole pairs can be formed (Ghaderi et al. 2015; Roozban et al. 2017a). The generated

electron–hole pairs have the ability to transfer to the surface and participate in redox reactions. Water and oxygen can react with the produced electron–hole pairs and form different types of oxidizing species (Ghaderi et al. 2018; Roozban et al. 2017b).

Due to the instability of the produced electron–hole pairs, they can easily recombine with each other and release energy. Therefore, the efficiency of the photocatalytic degradation can be decreased (Ahmad et al. 2014; Zhu et al. 2003). Several methods have been investigated to decline the recombination rate of the electron–hole pair as well as increment the photocatalytic removal efficiency. The most important principle in this field is the significant separation of the generated electrical charges. Connection of semiconductors with wide band gap on the surface of the semiconductor, photocatalytic semiconductor connection on materials with high surface to volume ratio including carbon nanotubes and graphene oxide (Abbasi 2021b; Abbasi et al. 2020; Byrappa et al. 2008; Gao and Sun 2014; Reddy et al. 2015) and also connection of noble metals such as gold and silver are effective methods for successful separation of the generated electron–hole pairs. Carbon nanotubes (CNTs), as

✉ Sedigheh Abbasi  
s.abbasi@esfarayen.ac.ir; abasi\_1362@yahoo.com

<sup>1</sup> Central Research Laboratory, Esfarayen University of Technology, Esfarayen, North Khorasan, Iran

most important member of the carbon material group, are single-walled (SW), double-walled (DW) and multi-walled (MW) (Abbasi et al. 2013; Abbasi et al. 2016). The unique properties of multi-walled carbon nanotubes (MWCNTs) such as high specific surface area, remarkable chemical stability, acceptable catalytic activity and non-toxicity have led to their wide application in energy storage, electrode fabrication and photocatalyst substrate (Byrappa et al. 2008; Abbasi et al. 2014). The application of MWCNTs in the structure of semiconductor photocatalysts increases the rate of photocatalytic activity and the destruction rate pollutants. The improvement of photocatalytic performance may be due to the facilitation of electron transfer from the conduction band of photocatalysts to MWCNTs (Abbasi and Hasanpour 2017a; Abbasi et al. 2017a). Therefore, this increases the electron–hole separation and decreases the recombination rate. According to recent reports, it is observed that ZnO, TiO<sub>2</sub> and SnO<sub>2</sub> are most used in photocatalytic process to remove contaminants. TiO<sub>2</sub> nanoparticles are considered by many researchers as photocatalysts due to suitable band gap and excellent photocatalytic activity. TiO<sub>2</sub> nanoparticles typically have several structures including anatase, rutile and brookite (Abbasi et al. 2015; Dastan 2017; Dastan et al. 2017). Studies show that the photocatalytic activity of each of these structures is not the same. In recent years, the photocatalytic activity of MWCNTs fused to single structure of TiO<sub>2</sub> nanoparticles has been investigated by many researchers. However, the photocatalytic activity of decorated MWCNTs with multiple structures of TiO<sub>2</sub> nanoparticles has not yet been investigated. Also, the effect of the amount of decorated TiO<sub>2</sub> nanoparticles on the surface of MWCNTs on the photocatalytic activity has not been investigated. Therefore, the purpose of this research is to synthesize TiO<sub>2</sub> nanoparticles with two structures of anatase and rutile on the surface of MWCNTs to investigate the amount of photocatalytic activity for destruction of methyl orange (MO). Meanwhile, the importance of main factors (such as pH of suspensions and irradiation time) affecting the removal of MO is studied using statistical analysis. The influence of different levels of effective parameters on the decomposition of MO as an organic pollutant has been studied based on Duncan's multiple range test.

## Experimental

### Materials

Materials used in this research including the following:

Tetra chloride titanium (TiCl<sub>4</sub>, 99%, Merck) as precursor of TiO<sub>2</sub> nanoparticles, MWCNTs (95.9% purity, diameter: ~40–60 nm, length: ~5–15 μm) is applied as substrate for synthesis of photocatalysts nanoparticles, Nitric Acid

(HNO<sub>3</sub>, *M* = 63, 65%, Merck) is used for treatment of pristine MWCNTs and producing the functionalized MWCNTs, and Methyl orange (99.5%, Merck) is applied to evaluate the photocatalytic activity of prepared photocatalysts.

### Synthesis of photocatalysts including MWCNTs and TiO<sub>2</sub>

The synthesis of the applied photocatalysts consists of two main steps. The first step is to prepare the hydrophobic MWCNTs for bonding the TiO<sub>2</sub> nanoparticles, and the second step is the synthesis of TiO<sub>2</sub> nanoparticles on the functionalized MWCNTs surface which is produced in the previous step. To perform the first step, follow the method presented in the previous article of this team (Abbasi et al. 2017a; Abbasi et al. 2015). In summary, 0.1 g of crude MWCNTs is dispersed on 50 mL of nitric acid and placed on a magnetic stirrer at 800 rpm for 2 h. Then, the container of acid nitric and MWCNTs is placed in the ultrasonic bath for 2 h. Finally, the suspension is subjected to filtration, rinsed several times with distilled water and dried at 90 °C for 12 h. The characterization of the dried MWCNTs using FTIR reveals that the surface of MWCNT is functionalized with functional groups includes oxygen such as OH and COOH. The results are presented in our previous work (Abbasi 2021a). The perform of the second step process, 0.08 g, of functionalized MWCNTs in the first step is pervaded in 100 mL of distilled water and placed in an ultrasonic bath for 30 min so that the functionalized MWCNTs are evenly dispersed in the distilled water. Then, in order to bind a certain amount of TiO<sub>2</sub> nanoparticles on the surface of functionalized MWCNTs, a certain amount of TiCl<sub>4</sub> (0.4 and 0.8 mL values are selected in this study) is added to the mixture containing distilled water and functionalized MWCNTs and placed on a stirrer under laboratory conditions for 5 h. Afterward, the temperature of the reaction mixture is increment until 60 °C and mixed at the same temperature for 12 h. Finally, the reaction mixture is filtered, washed and heated in an oven at 350 °C for 3 h. The synthesized photocatalysts containing 0.4 and 0.8 mL TiCl<sub>4</sub> are named as MCT#1 and MCT#2, respectively.

### Evaluation of contaminant removal efficiency using MCT#1 and MCT#2

A reactor equipped with a UV lamp (150W) is used to evaluate the photocatalytic activity of prepared MCT#1 and MCT#2. To ensure uniform irradiation of the solution containing MO, try to place the UV lamp exactly in the center of the reactor. Due to the gradual increase in temperature of suspensions that is related to the presence of UV lamp, the reactor is equipped with a water circulation to keep the temperature constant during the reaction. The influence

of two effective factors (pH and irradiation time) on MO destruction is studied. The range of pH changes is 3–11, and the range of time changes is up to 35 min. for experiment, 80 mL of aqueous solution with a concentration of 10 ppm of MO is prepared. In all of experiment, the concentration of MCT#1 and MCT#2 is kept constant at 0.2%wt and the pH of suspensions is adjusted to 3, 7 and 11 using a solution of hydrochloric acid and sodium hydroxide. Each container involving the synthesized photocatalysts and MO that is set at a specific pH is mixed in a dim box for 1 h to adsorption–desorption equilibrium. After equilibration, the suspension is irradiated and every 5 min, and 3 mL of suspension is drained and passed through filter paper several times to remove the applied samples. Then, the output of filter is analyzed using a spectrophotometer (Perkin Elmer Company) at 464 nm to measure the absorbance. The amount of adsorption measured at each time interval is considered as  $A_t$ . In general, the amount of adsorption measured depends directly on the contaminant concentration in the suspensions. Therefore, with increasing the concentration on pollutants, the amount of absorption also increases. Finally, the amount of destruction rate of the MO using synthesized MCT#1 and MCT#2 is calculated using the Eq. 1 (Abbasi s et al. 2019; Abbasi et al. 2017b):

$$(\text{destruction rate})^{-1} = \frac{C_t}{C_0} \quad (1)$$

### Analysis of variance (ANOVA)

The effect of studied parameters (pH and irradiation time) and their interactions on the destruction rate of MO using synthesized MCT#1 and MCT#2 is investigated using analysis of variance (ANOVA). The ANOVA Tables are prepared using design of experiments (DOE) software version 6.0.2. The applied level of probability in this study is considered 5% ( $\alpha = 0.05$ ). To increase the precision of the results, whole tests are repeated three times and their mean is expressed as the result. Duncan's multiple range test using MSTAT-C software (Ver 1.42) is used to study the effect of different levels of changes in the main factors on destruction rate of pollutant.

## Results and discussion

### XRD analysis

XRD diffraction patterns of the prepared MCT#1 and MCT#2 are illustrated in Figs. 1 and 2, respectively. Insets in these two Figures confirm the attendance of the crystal structure of TiO<sub>2</sub> nanoparticles. The results of the XRD

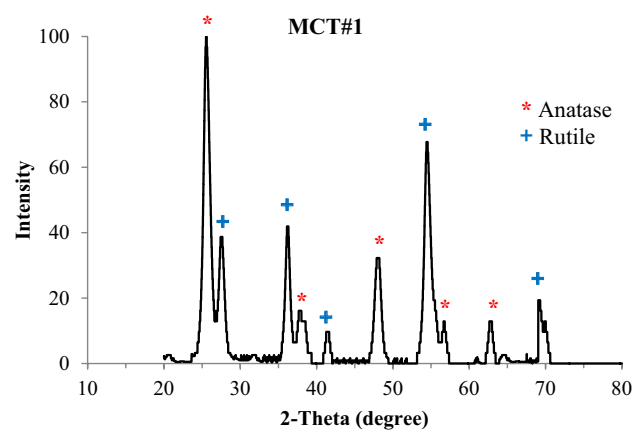


Fig. 1 XRD pattern of the synthesized MCT#1

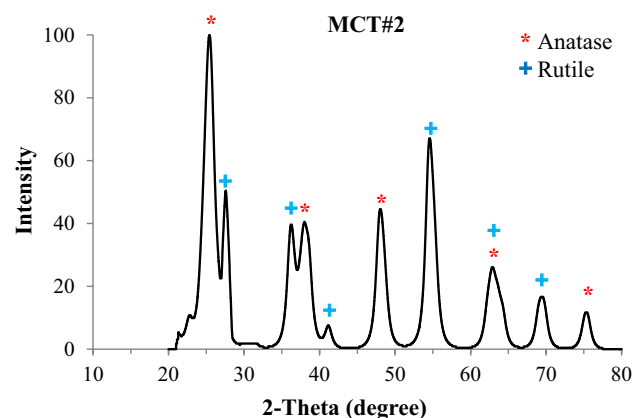
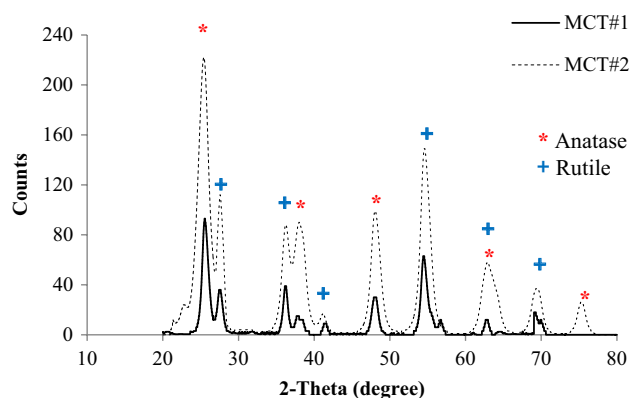


Fig. 2 XRD pattern of the synthesized MCT#2

patterns confirm that the synthesized TiO<sub>2</sub> nanoparticles have both tetragonal anatase structure and tetragonal rutile structure. The detectable peaks at 25.43°, 37.80°, 48.20° and 62.81° are appointed to (101), (004), (200) and (204) reflection of anatase phase of TiO<sub>2</sub> nanoparticles, respectively. Meanwhile, the observed peaks at around 27.47°, 36.20°, 41.44°, 54.37°, 62.8° and 68.86° are assigned to the (110), (101), (111), (211), (002) and (204) reflection of rutile phase of TiO<sub>2</sub> nanoparticles, respectively. However, in the both of MCT#1 and MCT#2, the fraction of the anatase phase is more than of rutile phase. The presence of sharp diffraction peaks in the XRD patterns of the synthesized MCT#1 and MCT#2 specifies that both formed crystal phases have acceptable crystallinity (Tharsika et al. 2014). The comparison between XRD patterns of MCT#1 and MCT#2 (Fig. 3) shows that the intension of principal peaks of anatase and rutile structures in MCT#1 is weaker than that of MCT#2. Therefore, it confirms that the level of decorated TiO<sub>2</sub> nanoparticles in the both phases in MCT#2 is higher than that of MCT#1. It is ascribed to volume of TiCl<sub>4</sub> that is applied



**Fig. 3** Comparison between XRD patterns of MCT#1 and MCT#2

during the preparation of TiO<sub>2</sub> nanoparticles. According to XRD patterns of MCT#1 and MCT#2, it is obvious that characteristic peak of graphite that is corresponded to the (002) reflection of MWCNTs is not observable. It may be attributed to the overlap of the (002) reflection of MWCNTs and (101) reflection of anatase phase of TiO<sub>2</sub> nanoparticles. The other reason may be due to the comprisable amount of anatase and MWCNTs.

### Photocatalytic activity study

Changes in MO destruction with irradiation time and pH in suspensions containing MCT#1 and MCT#2 can be observed in Figs. 4 and 5, respectively. Based on results, it is observed that with increasing exposure time of the suspensions containing methyl orange and the used photocatalysts, the methyl orange concentration is reduced compared to the initial concentration. However, the lowest concentration of methyl orange occurs after 35 min of irradiation. Therefore, the effect of increasing irradiation time on methyl orange degradation and decrease in pollutant concentration can

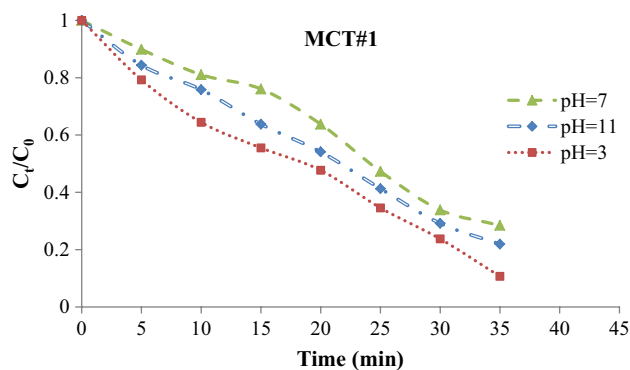


**Fig. 4** Changes in MO destruction with irradiation time and pH in the suspension containing MCT#1 as photocatalyst

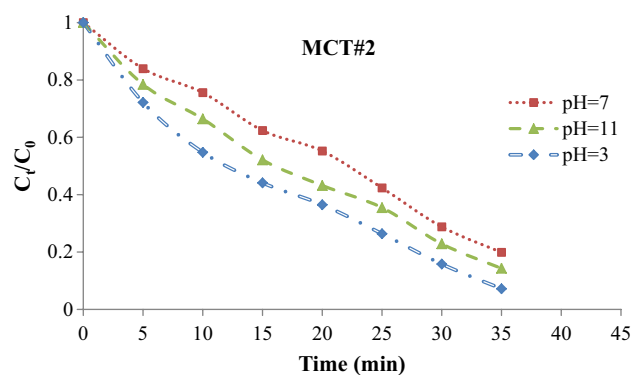


**Fig. 5** Changes in MO destruction with irradiation time and pH in the suspension containing MCT#2 as photocatalyst

be deduced. By exposing the photocatalyst to UV ray, the valence layer electrons can be stimulated and move to the conduction layer. Electron transfer from the valence layer to the conduction layer causes a hole in the valence layer and an electron in the conduction layer (Abbasi 2021a; Abbasi and Hasanpour 2017b). An increase in electron excitation causes an increase in the rate of electron transfer as well as the number of produced electrons and holes pairs. Because the created electrons and holes have a significant role in the decomposition of dye contaminants, increasing the irradiation time increments the degradation of the organic pollutants and decreases the concentration. In fact, the produced electrons can react with oxygen to form oxygen radicals. Then, these radicals can convert to the hydrogen peroxide (H<sub>2</sub>O<sub>2</sub>). Subsequently, the reaction between H<sub>2</sub>O<sub>2</sub> and electron causes to the formation of hydroxyl radicals (OH<sup>•</sup>) (Abbasi et al. 2021). Finally, the formed radicals can successfully destruct the organic contaminant such as MO. The presence of MWCNTs improves the separation of produced electron–hole pairs, and this increases the photocatalytic activity for degradation of MO (Abbasi and Hasanpour 2017a; Wang Yao and Li 2009). Examination of the changes of methyl orange concentration with pH indicates that with the change of pH, the MO concentration also changes substantially, while the highest and lowest destruction rate of MO (in the same conditions in terms of radiation time) are occurred in the acidic (pH = 3) and neutral (pH = 7) mediums, respectively. Therefore, the final concentration of MO in acidic condition is lower than that of neutral suspension. This is because of the influence of the presence of hydrogen ions (H<sup>+</sup>) in the acidic medium on the decomposition of methyl orange. The hydrogen ions that are presented in the acidic medium are capable of absorbing electrons and producing the hydrogen radicals. Then, the hydrogen radicals can successfully produce the hydroxyl radicals that play a significant role in destruction of pollutant (Abbasi et al. 2017a; Abbasi and Hasanpour 2017b; Kim et al. 2015).

Therefore, it can be confirmed that the decomposition of MO can be enhanced by increasing the hydrogen ions and decreasing the pH of suspension. The lower degradation rate of methyl orange in neutral conditions is related to the effect of surface charges on the photocatalyst surface. The enhancement of surface charge causes the augmentation of photocatalyst dispersion in suspension. Therefore, the probability of the photocatalyst being exposed to UV radiation is significantly increased. Thus, the amount of produced electron–hole pairs can be enhanced. Therefore, because the surface charge on the photocatalysts in the neutral medium is much lower, the degradation rate of methyl orange in neutral conditions is lower than that of acidic and alkaline conditions. A schematic of the photocatalytic process is shown in the Fig. 6.

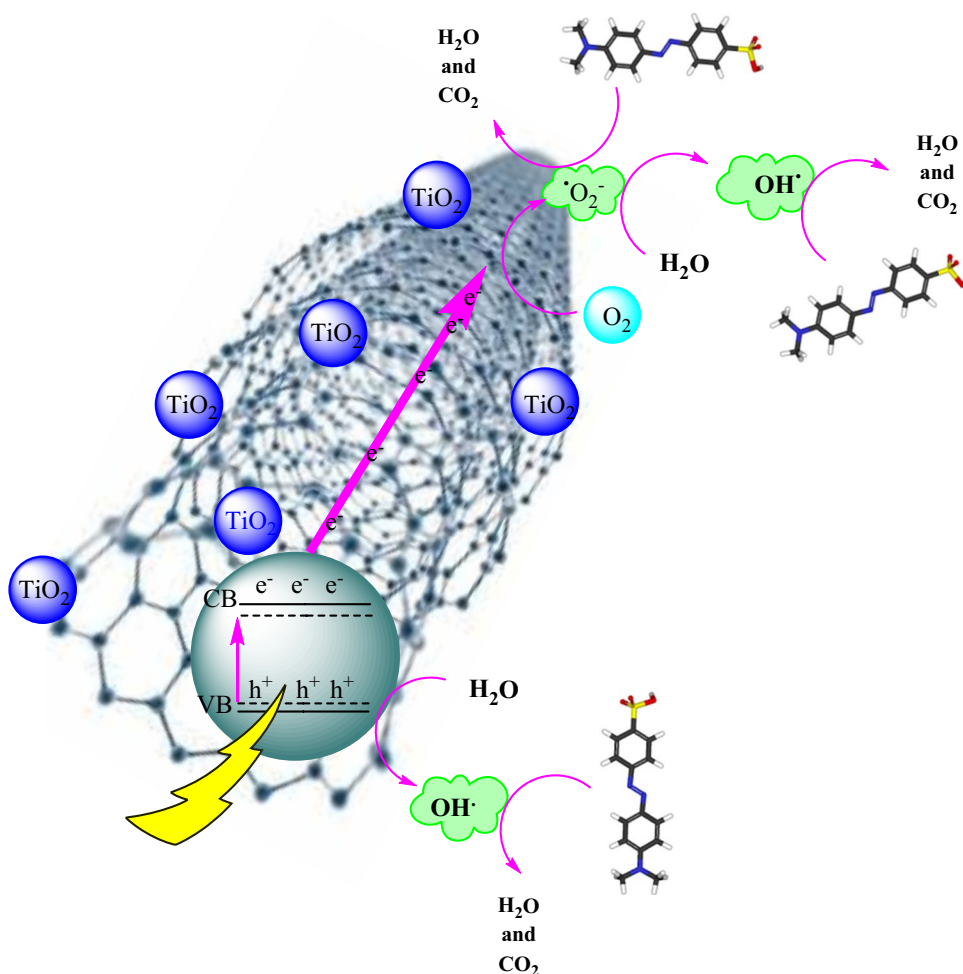
Figure 7 illustrates the comparison between MO concentration changes over time by MCT#1 and MCT#2 at distinct pH. The results show that at all of studied pH (pH = 3, pH = 7 and pH = 11), the synthesized MCT#2 has higher destruction rate rather than MCT#1. It can be related to the effect of TiO<sub>2</sub> nanoparticles content that is presented in synthesized photocatalysts. Since the amount of TiO<sub>2</sub>

nanoparticles in synthesized MCT#2 is higher compared to MCT#1, the amount of generated oxidizing radicals in synthesized MCT#2 is also higher than that of MCT#1. Therefore, it can be deduced that the amount of TiO<sub>2</sub> nanoparticles attached to MWCNTs surface is an important factor in the destruction rate of MO.

### ANOVA study

The results of statistical analysis according to ANOVA for decomposition of MO using synthesized MCT#1 and MCT#2 are listed in Tables 1 and 2, respectively. According to the applied levels of investigated parameters, the degree of freedom (Df) of time and acidity is determined as 6 and 2. In fact, the degree of freedom of each factor that is checked is one less than the number of levels of the same factor. The *F*-values show the importance and impact of each factor on the MO removal efficiency. Therefore, the factors with higher *F*-values have a greater effect on the pollutant removal (Ekrami-Kakhki et al. 2018; Namvar-Mahboub and Pakizeh 2014). According to the values presented in the Table1, it can be seen that the *F*-values for

**Fig. 6** A schematic of the photocatalytic process of MCT#1 and MCT#2



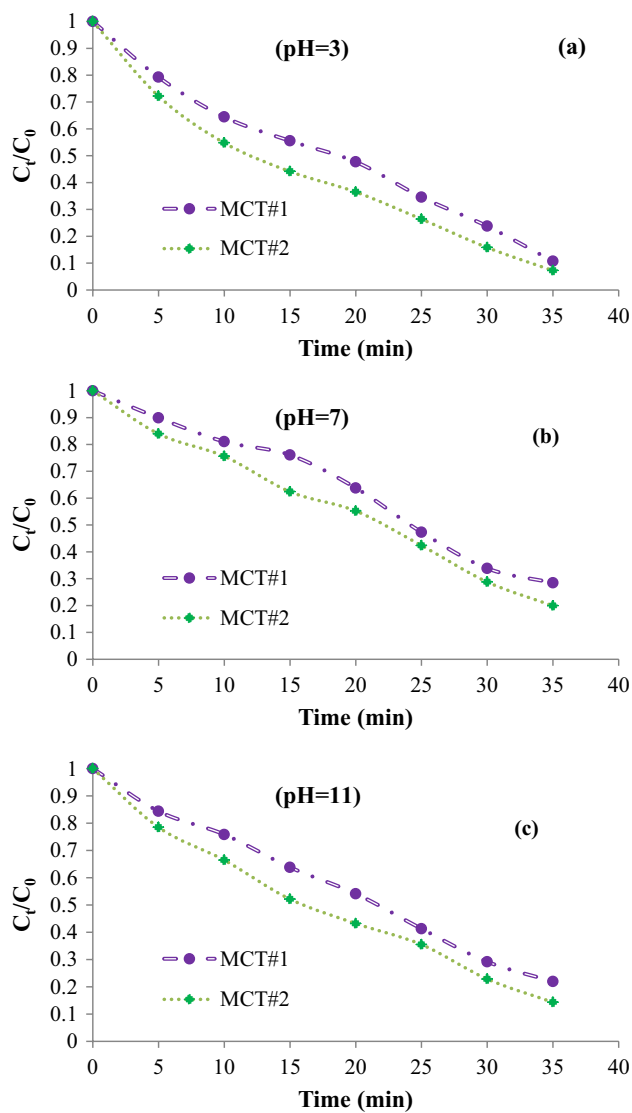


**Fig. 7** Comparison between MO concentration changes over time using MCT#1 and MCT#2, at distinct pH, **a:** pH=3, **b:** pH=7, **c:** pH=11

the irradiation time, pH and their interactions are equal to 12,331.88, 2924.52 and 16.23, respectively. Thus, it may be concluded that the irradiation time has a greater influence

on degradation of MO than acidity as well as their interaction. By studying the results presented in Table 2, it can be seen that similar results are obtained for pollutant removal using the MCT#2. So that the use of the MCT#2 as a photocatalyst causes the F-value for the irradiation time, pH and their interactions to become 8858.28, 1822.33 and 18.57, respectively. p value is another statistical parameter that can be used to determine the effectiveness of the investigated factors as well as their mutual interaction on the removal efficiency of MO. Single parameters as well as their interactions that have an p value lower than the confidence level used in the statistical analysis (0.05) are known as parameters that have a significant effect on the response (Abbasi 2021a). Therefore, the examination of the p values presented in Tables 1 and 2 indicates that the individual parameters (A and B) as well as their interaction (A – B) have the p value of less than 0.05. Therefore, it can be confidently stated that all of investigated parameters have a significant influence on destruction of MO using both of MCT#1 and MCT#2. The statistical parameter of lack of fit indicates the presence or absence of non-significant parameters in the presented model. This can be recognized using its degree of freedom. Visible values for lack of fit in Tables 1 and 2 show that the degree of freedom is equal to zero. Thus, it is safely concluded that both presented models include only effective parameters. Therefore, the values predicted by these two models have a very good agreement with the obtained experimental values.

The validity and adequacy of the presented models using MCT#1 and MCT#2 can be evaluated by the statistical parameters listed in Table 3. The most widely used statistical parameter that is used to check the adequacy of the model is the correlation coefficient ( $R^2$ ). The closer the correlation coefficient is to one, it indicates that the presented model has the ability to predict more realistic values. The  $R^2$  values of MCT#1 and MCT#2 models are equal to 99.96 and 99.93, respectively. Therefore, it derived that the variations of MO destruction rate with irradiation time and pH can be predicted with an accuracy of 99.90% with both models. Another statistical parameter presented in Table 3 is Adjusted  $R^2$  ( $R^2_{adj}$ ). The comparison between the  $R^2$  and  $R^2_{adj}$  parameters is a suitable criterion to determine the

**Table 1** Analysis of variance for MO destruction rate by MCT#1

Source	Sum of square	Df	Mean squares	F-Value	p value	
Model	3.21	20	0.16	4001.75	<0.0001	significant
A (Time)	2.97	6	0.49	12,331.88	<0.0001	significant
B (pH)	0.23	2	0.12	2924.52	<0.0001	significant
AB	7.81E-03	12	6.50E-04	16.23	<0.0001	significant
Lack of fit	0	0	–	–	–	not significant
Pure error	1.68E-03	42	4.01E-05	–	–	–
Total	3.21	62	–	–	–	–

**Table 2** Analysis of variance for MO destruction rate by MCT#2

Source	Sum of Square	Df	Mean Squares	F-Value	p value	
Model	2.57	20	0.13	2850.86	<0.0001	significant
A (Time)	2.40	6	0.40	8858.28	<0.0001	significant
B (pH)	0.16	2	0.082	1822.33	<0.0001	significant
AB	0.01	12	8.38E-04	18.57	<0.0001	significant
Lack of fit	0	0	–	–	–	not significant
Pure error	1.89E-03	42	4.51E-05	–	–	–
Total	2.58	62	–	–	–	–

**Table 3** Effective factors in the adequacy of the proposed models

The proposed model using photocatalyst	$R^2\%$	Adjusted $R^2 (R^2_{adj})\%$	Predicted $R^2 (R^2_{pred})\%$	Adequate precision
MCT#1	0.9996	0.9991	0.9985	204.605
MCT#2	0.9993	0.9989	0.9983	183.031

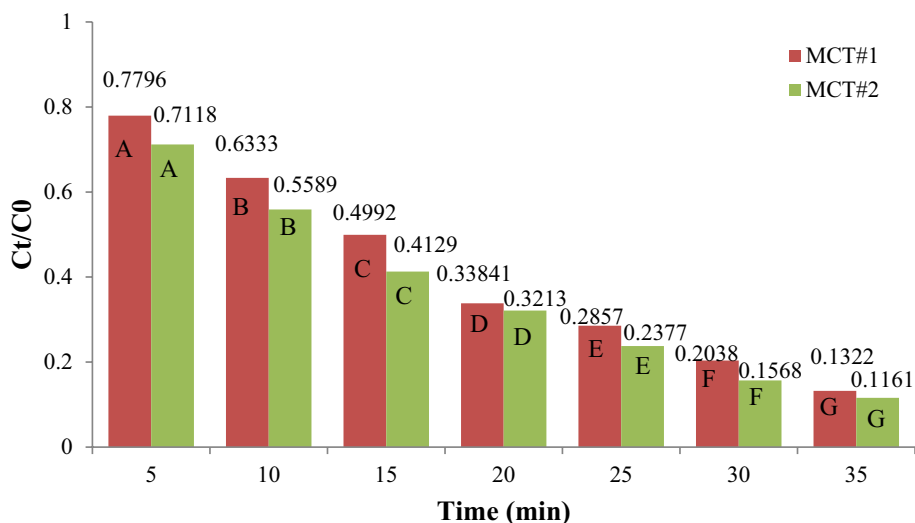
suitability of the presented models. So that in the models that have the highest level of adequacy, the amount of  $R^2$  and  $R^2_{adj}$  does not have a significant difference and the difference of these two statistical parameters can be ignored (Abbasi et al. 2020). The  $R^2_{adj}$  values related to MCT#1 and MCT#2 models are 99.91 and 99.89, respectively. Therefore, as can be seen, the difference between  $R^2$  and  $R^2_{adj}$  in MCT#1 and MCT#2 models is 0.05 and 0.04, respectively. Therefore, considering that the difference between these two values is very small, the adequacy of the model can be confirmed and it is stated that the proposed models only contain main factors. Predicted  $R^2 (R^2_{pred})$  is another statistical parameter that is used to measure the adequacy of the models. In high-quality models, the difference between  $R^2_{adj}$  and  $R^2_{pred}$  should not be more than 0.2. According to the results of

Table 3, it is obvious that the discrepancy among these two factors in the both models is less than 0.2. Thus, the values of  $R^2_{pred}$  are confirmed the adequacy of the models. The adequate precision value indicates the ratio of the actual value to the fluctuation. If this ratio is more than 4, it can be concluded that the amount of fluctuations is low compared to the real values (Abbasi and Hasanpour 2017b). According to the results, it can be seen that therefore, the adequate precision values for both of MCT#1 and MCT#2 models are higher than 4. Therefore, these parameters also affirm the suitability of the models.

**Duncan’s multiple range test study**

The statistical results of MO degradation rate according to Duncan’s multiple range test are demonstrated in Figs. 8 and 9. The effect of seven levels of irradiation time on destruction rate of MO by MCT#1 and MCT#2 is presented in Fig. 8. It is obvious that the contaminant concentration decreases dramatically with increasing the irradiation time. This is due to the influence of irradiation time on the quantity of oxidizing radicals. In fact, as the irradiation time increases, the number of excited electrons that are transferred from the valence band to the conduction band

**Fig. 8** Investigation of destruction rate changes of MO with irradiation time (at constant pH) using MCT#1 and MCT#2 based on Duncan’s multiple range test at  $\alpha = 0.05$



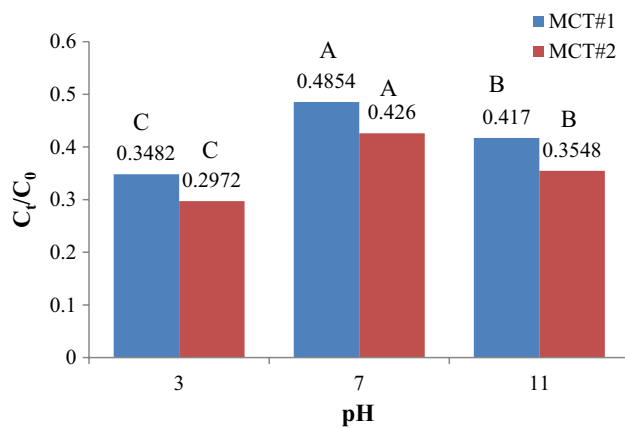


**Fig. 9** Investigation of destruction rate changes of MO with pH (at constant irradiation time) using MCT#1 and MCT#2 based on Duncan's multiple range test at  $\alpha = 0.05$

increases (Abbasi 2021a, 2021b). It can also be seen that the decrease in pollutant concentration in the presence of MCT#1 is less compared to MCT#2. It can be attributed to the amount of semiconductor nanoparticles ( $\text{TiO}_2$ ) in MCT#1 and MCT#2. The presented results in Fig. 8 reveal that all seven levels of irradiation time have a significant influence ( $\alpha = 0.05$ ) on the MO concentration.

The changes of MO concentration with pH of suspension containing MCT#1 and MCT#2 are shown in Fig. 9. It is clear that based on Duncan's multiple range test ( $\alpha = 0.05$ ), three studied levels of pH (3, 7 and 11) have a significant effect on the concentration of MO. Meanwhile, it can be observed that the MO concentration in the suspension containing MCT#1 is higher than that of MCT#2. The high level of contaminant in the suspension containing MCT#1 is due to the low amount of photocatalytic  $\text{TiO}_2$  nanoparticles in the synthesized photocatalyst. Reducing the amount  $\text{TiO}_2$  nanoparticles cause the number of electron-hole pairs, so the number of radicals that is affected in the decomposition of the pollutant is also reduced (Abbasi 2019; Abbasi et al. 2020). The results of Fig. 9 corroborate that the most and the least destruction rate of MO using both of MCT#1 and MCT#2 are at pH = 3 and pH = 7, respectively. The results confirm the effect of pH on the concentration of pollutants base on previous reports (Abbasi and Hasanpour 2017a).

## Conclusions

In the present research, the effect of photocatalysts including MWCNTs and  $\text{TiO}_2$  nanoparticles on the reduction in MO concentration is investigated. According to the results, it is found that both synthesized photocatalysts have a reasonable influence on destruction of MO from aquatic system. MO concentration enhances with augmentation of irradiation

time in the presence of both MCT#1 and MCT#2. The significant effect of the all studied levels of main factors such as pH and irradiation time is confirmed using statistical analysis of results based on Duncan's multiple range test.

**Acknowledgements** The support of the officials of Esfarayen University of Technology as well as the director of the Central Research Laboratory is extremely appreciated.

**Funding** The author(s) received no specific funding for this work

## Declarations

**Conflict of interest** The authors of this article undertake that they have no financial and personal relationships with any other individuals or entities that could adversely affect their research.

**Open Access** This article is licensed under a Creative Commons Attribution 4.0 International License, which permits use, sharing, adaptation, distribution and reproduction in any medium or format, as long as you give appropriate credit to the original author(s) and the source, provide a link to the Creative Commons licence, and indicate if changes were made. The images or other third party material in this article are included in the article's Creative Commons licence, unless indicated otherwise in a credit line to the material. If material is not included in the article's Creative Commons licence and your intended use is not permitted by statutory regulation or exceeds the permitted use, you will need to obtain permission directly from the copyright holder. To view a copy of this licence, visit <http://creativecommons.org/licenses/by/4.0/>.

## References

- Abbasi S (2018) Investigation of the enhancement and optimization of the photocatalytic activity of modified  $\text{TiO}_2$  nanoparticles with  $\text{SnO}_2$  nanoparticles using statistical method. *Mater Res Express* 5:066302
- Abbasi S (2019) Photocatalytic activity study of coated Anatase-Rutile Titania nanoparticles with nanocrystalline tin dioxide based on the statistical analysis. *Environ Monit Assess* 191(4):206–218
- Abbasi S (2020) Adsorption of dye organic pollutant using magnetic ZnO embedded on the surface of graphene oxide. *J Inorg Organomet Polym Mater* 30:1924–1934
- Abbasi S (2021a) The degradation rate study of methyl orange using MWCNTs@ $\text{TiO}_2$  as photocatalyst, application of statistical analysis based on fisher's F distribution. *J Clust Sci* 33(2):593–602
- Abbasi S (2021b) Response surface methodology for photo degradation of methyl orange using magnetic nanocomposites containing zinc oxide. *J Clust Sci* 32(4):805–812
- Abbasi S, Hasanpour M (2017a) Variation of the photocatalytic performance of decorated MWCNTs (MWCNTs-ZnO) with pH for photo degradation of methyl orange. *J Mater Sci: Mater Electron* 28(16):11846–11855
- Abbasi S, Hasanpour M (2017b) The effect of pH on the photocatalytic degradation of methyl orange using decorated ZnO nanoparticles with  $\text{SnO}_2$  nanoparticles. *J Mater Sci: Mater Electron* 28(2):1307–1314
- Abbasi S, Zebarjad SM, Baghban SHN (2013) Decorating and filling of multi-walled carbon nanotubes with  $\text{TiO}_2$  nanoparticles via wet chemical method. *Engineering* 5:207–212
- Abbasi S et al (2014) Statistical analysis of thermal conductivity of nanofluid containing decorated multi-walled carbon nanotubes with  $\text{TiO}_2$  nanoparticles. *Bull Mater Sci* 37(6):1439–1445



- Abbasi S et al (2015) Synthesis of TiO<sub>2</sub> nanoparticles and decorated multiwalled carbon nanotubes with various content of rutile titania. *Synth React Inorg, Met-Org, Nano-Met Chem* 45:1539–1548
- Abbasi S et al (2016) Experimental investigation of the rheological behavior and viscosity of decorated multi-walled carbon nanotubes with TiO<sub>2</sub> nanoparticles/water nanofluids. *J Therm Anal Calorim* 123:81–89
- Abbasi S, Hasanpour M, Kakhki MSE (2017a) Removal efficiency optimization of organic pollutant (methylene blue) with modified multi-walled carbon nanotubes using design of experiments (DOE). *J Mater Sci: Mater Electron* 28(13):9900–9910
- Abbasi S, Ekrami-Kakhki M-S, Tahari M (2017b) Modeling and predicting the photodecomposition of methylene blue via ZnO-SnO<sub>2</sub> hybrids using design of experiments (DOE). *J Mater Sci: Mater Electron* 28(20):15306–15312
- Abbasi S, Ekrami-KakhkiTahari MSM (2019) The influence of ZnO nanoparticles amount on the optimisation of photo degradation of methyl orange using decorated MWCNTs. *Progress in Ind Ecol: Int J* 13(1):3–15
- Abbasi S et al (2020) Synthesis of magnetic Fe<sub>3</sub>O<sub>4</sub>@ZnO@graphene oxide nanocomposite for photodegradation of organic dye pollutant. *Int J Environ Anal Chem* 100(2):225–240
- Abbasi S et al (2021) Application of the statistical analysis methodology for photodegradation of methyl orange using a new nanocomposite containing modified TiO<sub>2</sub> semiconductor with SnO<sub>2</sub>. *Int J Environ Anal Chem* 101(2):208–224
- Ahmad M et al (2014) Photocatalytic, sonocatalytic and sonophotocatalytic degradation of Rhodamine B using ZnO/CNTs composites photocatalysts. *Ultrason Sonochem* 21(2):761–773
- Byrappa K et al (2008) Hydrothermal preparation of ZnO:CNT and TiO<sub>2</sub>:CNT composites and their photocatalytic applications. *J Mater Sci* 43:2348–2355
- Dastan D (2017) Effect of preparation methods on the properties of titania nanoparticles: solvothermal versus sol–gel. *Appl Phys A* 123(11):699–711
- Dastan D, Chaure N, Kartha M (2017) Surfactants assisted solvothermal derived titania nanoparticles: synthesis and simulation. *J Mater Sci: Mater Electron* 28:7784–7796
- Ekrami-Kakhki M-S, Abbasi S, Farzaneh N (2018) Statistical analysis of the electrocatalytic activity of Pt nanoparticles supported on novel functionalized reduced graphene oxide-chitosan for methanol electrooxidation. *Electron Mater Lett* 14(1):70–78
- Gao P, Sun DD (2014) Hierarchical sulfonated graphene oxide–TiO<sub>2</sub> composites for highly efficient hydrogen production with a wide pH range. *Appl Catal B-Environ* 147:888–896
- Ghaderi A, Abbasi S, Farahbod F (2015) Synthesis of SnO<sub>2</sub> and ZnO Nanoparticles and SnO<sub>2</sub>-ZnO Hybrid for the photocatalytic oxidation of methylene orange. *Iran J Chem Eng* 12(3):96–105
- Ghaderi A, Abbasi S, Farahbod F (2018) Synthesis, characterization and photocatalytic performance of modified ZnO nanoparticles with SnO<sub>2</sub> nanoparticles. *Mater Res Express* 5:065908
- Kim SP, Choi MY, Choi HC (2015) Characterization and photocatalytic performance of SnO<sub>2</sub>-CNTnanocomposites. *Appl Surf Sci* 357:302–308
- Namvar-Mahboub M, Pakizeh M (2014) Optimization of preparation conditions of polyamide thin film composite membrane for organic solvent nanofiltration. *Korean J Chem Eng* 31(2):327–337
- Reddy DA, Ma R, Kim TK (2015) Efficient photocatalytic degradation of methylene blue by heterostructured ZnO–RGO/RuO<sub>2</sub> nanocomposite under the simulated sunlight irradiation. *Ceram Int* 41:6999–7009
- Roosban N, Abbasi S, Ghazizadeh M (2017a) The experimental and statistical investigation of the photo degradation of methyl orange using modified MWCNTs with different amount of ZnO nanoparticles. *J Mater Sci: Mater Electron* 28(10):7343–7352
- Roosban N, Abbasi S, Ghazizadeh M (2017b) Statistical analysis of the photocatalytic activity of decorated Multi-Walled carbon nanotubes with ZnO nanoparticles. *J Mater Sci: Mater Electron* 28(8):6047–6055
- Tharsika T et al (2014) Enhanced ethanol gas sensing properties of SnO<sub>2</sub>-Core/ZnO-shell nanostructures. *Sensors* 14:14586–14600
- Wang X, Yao S, Li X (2009) Sol-gel preparation of CNT/ZnO nanocomposite and its photocatalytic property. *Chin J Chem* 27:1317–1320
- Zhou N et al (2013) TiO<sub>2</sub> coated Au/Ag nanorods with enhanced photocatalytic activity under visible light irradiation. *Nanoscale* 5(10):4236–4241
- Zhu J et al (2003) Improving the dispersion and integration of single-walled carbon nanotubes in epoxy composites through functionalization. *Nano Lett* 3:1107–1113
- Zhu G et al (2015) A facile synthesis of ZnO/CNTs hierarchical microspheres composites with enhanced photocatalytic degradation of methylene blue. *RSC Adv* 5(89):72476–72481

**Publisher's Note** Springer Nature remains neutral with regard to jurisdictional claims in published maps and institutional affiliations.